Manganese clusters: a common ground for photosynthesis, quantum tunnelling of the magnetization and colossal magnetoresistance *

Andrea Caneschi, Dante Gatteschi and Roberta Sessoli

Department of Chemistry, University of Florence, Florence, Italy

Mixed-valence manganese clusters are briefly reviewed, showing their relevance to such diverse fields as metalloenzymes and metalloproteins, single-molecule magnets, and colossal magnetoresistance. Particular emphasis has been given to the possibility of using high-field EPR spectroscopy for obtaining structural information from EPR-silent ions such as manganese(III). Besides the small clusters, comprising two–four metal ions relevant to biological systems, a large interest is invested in larger clusters, with the aim of showing how synthetic work aimed at obtaining models for biological clusters has provided many interesting results for other types of investigations.

Clusters comprising mixed-valent transition-metal ions are present in several metalloenzymes and metalloproteins, ranging from iron–sulfur proteins to the water oxidizing complex, WOC, of Photosystem II of bacterial photosynthesis. Mixed-valence chemistry is particularly rich for manganese, because it can be stable in at least the +II, +III and +IV oxidation states.[1] This potential has been fully exploited by nature not only in the above mentioned WOC,[2] where all the possible oxidation states are present, but also in catalases,[3] bacterial ribonucleotide reductase,[4] *etc.*

The magnetic coupling between the mixed-valent species may provide useful tools for the investigation of the structures of the centres, both from direct magnetization measurements and from indirect spectroscopic investigations. The latter have been particularly exploited, also taking advantage of the comparison of the properties of simple model systems. The magnetic properties of manganese clusters are important not only for their biological relevance, but also because they have been found to behave as single-molecule magnets at low temperature.[5] Further these systems have been shown to undergo quantum tunnelling of the magnetization,[6] which is currently much investigated, also with the aim of finding suitable new materials for the development of future quantum computers. Finally mixed-valence Mn^{III}–Mn^{IV} perovskites are actively investigated[7] because they have been found to change dramatically their electric resistance in the presence of an applied magnetic field, giving rise to the so called colossal magnetoresistance.[8]

We feel that an overview of the relevance of simple manganese clusters to such diverse fields can be of interest and potentially cross fertilizing. We will briefly review the fundamentals of magnetic interactions between pairs of manganese ions, and then focus on large clusters, comprising four to twelve manganese ions. The former have been thoroughly investigated in connection with Photosystem II while the latter are currently under intense investigation as possible candidates for single-molecule magnets. We will not attempt to cover the whole field, but rather to work through some examples. Further we limit ourselves to mixed-valent species.

Electronic Structure of Manganese Ions

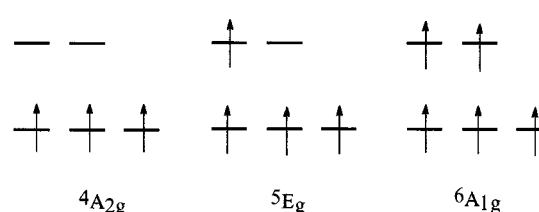The electron configurations of the three high-spin manganese ions in octahedral symmetry are shown in Fig. 1. Both

Fig. 1 Ground electronic configurations of octahedrally co-ordinated manganese ions in oxidation states IV (left), III (centre) and II (right)
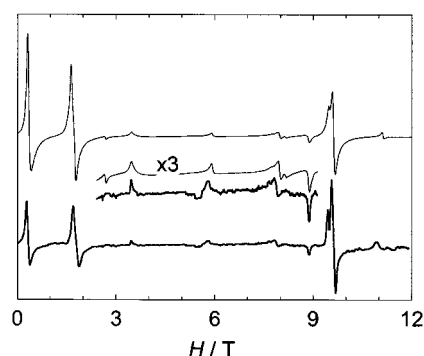

Fig. 2 High field EPR spectrum of a polycrystalline powder of [Mn(dbm)₃] recorded at 350 GHz and 15 K. The thicker lines correspond to the experimental spectrum, the others to the computer simulated with the parameters reported in the text

manganese(II) and manganese(IV), which are characterized by odd numbers of unpaired electrons, and usually do not have large zero field splitting effects, easily give EPR spectra, and this is indeed a very powerful tool for the spectroscopic investigation of the local environment of these ions in the clusters. Unfortunately much less is known of manganese(III), because this ion has an even number of unpaired electrons, and in octahedral symmetry it undergoes large Jahn–Teller distortions, which determine large zero field splittings. These two factors make manganese(III) essentially EPR silent in a conventional spectrometer, with the only exception being a broad feature which in some cases is observed at very low field.[9] This feature, which is similar to an analogous one observed in iron(II) complexes,[10] has been attributed to the forbidden $-2 \longrightarrow +2$ transition in lower than axial symmetry. However the recent introduction of high frequency EPR, HF-EPR, spectrometry is about to rapidly change the situation because in this case the spectra of manganese(III) compounds can be easily observed. Fig. 2 shows the EPR spectrum[11] of [Mn(dbm)₃], where dbm is 1,3-diphenylpropane-1,3-dione, recorded with an

exciting frequency of 350 GHz. Manganese(III) has the elongated octahedral co-ordination which is typical of this ion. Under these conditions it must be expected that the e_g levels are split, z^2 lying lowest. Therefore the ground configuration is (xz, yz, xy, z^2). In the spectra of Fig. 2 many transitions, corresponding to the fine structure of the ground $S = 2$ state, are observed. Since no obvious regularity is observed in the spacing between the lines it must be concluded that the zero field splitting, $(2S - 1)D$, is comparable to the microwave quantum of *ca.* 12 cm^{-1}. The spectra were satisfactorily fitted with a model which diagonalizes the full Hamiltonian matrix comprising the Zeeman and zero field terms $H = \mu_B \, \mathbf{H} \cdot \mathbf{g} \cdot \mathbf{S} + \mathbf{S} \cdot \mathbf{D} \cdot \mathbf{S}$. The best fit parameters are: $g_x = g_y = 1.99$, $g_z = 1.97$; $D = -4.35$ cm^{-1}, $E = 0.26$ cm^{-1}. It is important to stress that the fitting easily provides the sign of D, due to the polarization effects of the intensity of the transitions which are associated with the large Zeeman energy of *ca.* 17 K of the HF-EPR experiment. This can be easily understood in the high field limit, *i.e.* when the Zeeman energy is much larger than the zero field splitting. In fact at low temperature only the transitions involving the lowest lying $M = -S$ level can be observed. For positive D the parallel transitions occur at high field and those perpendicular at low field, while for negative D they are reversed.

The obtained spin Hamiltonian parameters could be analysed using a theoretical model based on ligand field theory. The g values are expected to be given by equation (1) where

$$g_z = g_e - \frac{8\lambda}{\Delta E(xy \longrightarrow x^2 - y^2)}; \, g_x = g_e - \frac{2\lambda}{\Delta E(yz \longrightarrow x^2 - y^2)};$$

$$g_y = g_e - \frac{2\lambda}{\Delta E(xz \longrightarrow x^2 - y^2)} \quad (1)$$

g_e is the free electron value, $\lambda = \zeta/2S$, ζ is the spin–orbit coupling constant, which for the free ion takes the value of 355 cm^{-1}, and ΔE is the energy difference between the indicated d orbitals. The analysis of the UV/VIS spectra suggests[13] that $\Delta E(xy \longrightarrow x^2 - y^2) = 18\,000$ cm^{-1}, $\Delta E(xz, yz \longrightarrow x^2 - y^2) = 21\,000$ cm^{-1}, which combined with equation (1) gives $g_x = g_y = 1.99$; $g_z = 1.96$, in excellent agreement with the experimental values. Analogous formulae can be calculated for the zero field splitting tensor. At the same level of approximation as in (1) the D and E parameters are given in equation (2). In this

$$D = \frac{1}{2}\lambda\left[g_z - \frac{1}{2}\left(g_x + g_y\right)\right]; \qquad E = \frac{1}{4}\lambda[g_x - g_y] \quad (2)$$

case the calculated value is $D = -0.9$ cm^{-1}, which has the right sign but is much smaller than the experimental value. In fact an additional contribution to D is given by the admixture of the ground state with the excited $^3T_{1g}$ originating from the t_{2g}^4 configuration. The contribution can be written as in equation (3),

$$D = -\frac{\zeta^2}{6B + 5C + \Delta E(xz, yz \longrightarrow z^2)} \quad (3)$$

where B and C are electron repulsion terms, which in the free ion take the values $B = 1140$ cm^{-1} and $C = 3675$ cm^{-1}. Including this additional contribution with $\Delta E(xy, yz \longrightarrow z^2)$ obtained from a ligand field analysis of the spectra the calculated $D = -5.3$ cm^{-1} is in very good agreement with experiment. It must be noticed that no orbital reduction factors were taken into account.

It is certainly very rewarding to see for the first time that indeed the spin Hamiltonian parameters of manganese(III) complexes can be easily reproduced with relatively simple perturbation formulae. This gives a hint that the hyperfine tensor, which so far has not been experimentally observed but indirectly obtained from the analysis of the spectra of pairs, can also be reasonably calculated using the perturbative ligand field approach. The corresponding formulae for the metal hyperfine

splitting, neglecting the orbit dipolar contributions, which are expected to be small due to the fact that the g values are very close to 2, are given[14] by equation (4) where $P = g_e g_N \mu_B \mu_N \langle r^{-3} \rangle$,

$$A_z = P\left[-\kappa + \frac{1}{7}\right]; \qquad A_{x,y} = P\left[-\kappa - \frac{1}{14}\right] \quad (4)$$

and κ is a number which expresses the Fermi contact term in units of P. Equation (4) shows that indeed the hyperfine coupling of manganese(III) has a sizeable anisotropy, due to dipolar terms. For instance for Mn^{3+} in rutile it was found[15] that $|A_z| = 53.10^{-4}$ cm^{-1}, $|A_{x,y}| = 83 \times 10^{-4}$ cm^{-1} and equation (4) was used to calculate $P = 140 \times 10^{-4}$ cm^{-1}, $\kappa = 0.52$. The value of P should be compared to that of the free ion, 212×10^{-4} cm^{-1}. The sign of the anisotropy is reversed in a compressed octahedral geometry. A similar reversed anisotropy can be expected in a trigonal-bipyramidal co-ordination, where there is also a hole in the z^2 orbital. This point has been recently raised in the interpretation of the EPR spectra of Photosystem II.[16]

Nature of the Exchange Interactions in Manganese Pairs

The exchange interactions in manganese pairs are expected to depend on several factors, including oxidation state, co-ordination geometry and exchange topology, valence localization *vs.* delocalization. A complete treatment should take into account all the above mentioned variables, trying to systematically generate all the possible cases. However this is clearly beyond the purposes of the present article, and only a brief overview will be given here, considering essentially pseudo-octahedral co-ordination environments around the metal ions. The first cases to be taken into account are the interactions between localized pairs mediated by superexchange interactions. In this case the sign and the extent of the interactions can be relatively easily understood using the Goodenough–Kanamori rules,[17] which state that the superexchange interactions between pairs of overlapping magnetic orbitals are antiferromagnetic, those between pairs of orthogonal magnetic orbitals are ferromagnetic. The overlap of the magnetic orbital of an ion with an empty orbital of another ion gives rise to ferromagnetic coupling through a spin polarization mechanism. In fact ferromagnetic coupling can also be observed in pairs containing manganese(III) ions, due to their peculiar configuration. In elongated octahedral co-ordination they have an empty $x^2 - y^2$ orbital, which can strongly interact with the bridging ligands through a σ^* mechanism. If the bridging ligand orbital can interact with a z^2 magnetic orbital of the other metal ion, the coupling is expected to be ferromagnetic. In fact a fraction of unpaired electron is transferred from the z^2 orbital on one side to the $x^2 - y^2$ orbital on the other side, and this, according to Hund's rule keeps the spin of the other unpaired electrons parallel to that in z^2.

In manganese(IV)–manganese(III) pairs there can be strong antiferromagnetic coupling originating from the interaction between the π^* orbitals of the two ions. All these pairs have been found to be strongly antiferromagnetically coupled, with J in the range 200–500 cm^{-1}, as shown in Table 1, where a selection of available experimental data is provided. In general the manganese(II)–manganese(III) interactions are weaker than the corresponding manganese(III)–manganese(IV) interactions. This is due to both the presence of two magnetic orbitals more in manganese(II) compared to manganese(IV), and this gives in general more available ferromagnetic pathways, and to stronger covalency effects observed on increasing the charge on the metal, thus providing stronger interactions.

The couplings involving manganese(II) and manganese(II) are usually much smaller, but they also tend to be antiferromagnetic. Weak interactions are also observed for manganese(III)–manganese(III) pairs, while larger antiferromagnetic couplings are observed for manganese(IV)–manganese(IV) pairs.

Table 1 Exchange interactions in oxo-bridged manganese pairs*

Cluster	Oxidation states	J/cm^{-1} $(H = JS_1S_2)$	$d(\mathrm{Mn{-}Mn})/\text{Å}$	$d(\mathrm{Mn{-}O})/\text{Å}$	$\mathrm{Mn{-}O{-}Mn}/°$	Ref.
$\mathrm{Mn_2O_2(pic)_4 \cdot MeCN}$	IV,IV	174	2.747	1.819	98.1	18
$[\mathrm{Mn_2O_2(phen)_4}]^{4+}$	IV,IV	288	2.748	1.797–1.805	99.5	19
$[\mathrm{Mn_2O_3(TMACN)_2}]^{2+}$	IV,IV	780	2.296	1.817–1.833	78.0, 78.2	20
$[\mathrm{(bispicen)MnO_2Mn(bispicen)}]^{4+}$	IV,IV	250	2.2672	1.810, 1.812	95.0	21
$[\mathrm{Mn_2O_2(N_3O\text{-}py)_2}]^+$	III,IV	302	2.656	1.784–1.822	94.0	22
$[\mathrm{Mn_2O_2(OAc)(TACN)_2}]^{2+}$	III,IV	440	2.588	1.808–1.817	91.1	23
$\mathrm{Mn_2O_2(OAc)Cl_2(bpy)_2}$	III,IV	228	2.667	1.793–1.843	94.4	24
$[\mathrm{(phen)_2Mn(\mu\text{-}O)_2Mn(phen)_2}]^{3+}$	III,IV	296	2.7	1.808, 1.820	96.0	19
$[\mathrm{(bpy)_2Mn(\mu\text{-}O)_2Mn(bpy)_2}]^{3+}$	III,IV	300	2.716	1.784, 1.856	96.6	25
$[\mathrm{(cyclen)MnO_2(cyclen)}]^{3+}$	III,IV	276	2.694	1.812, 1.823	95.7	26
$[\mathrm{Mn_2O_2(O_2CCH_3)(bpea)_2}]^{2+}$	III,IV	328	2.6333	1.772, 1.791	92.4, 93.4	27
$[\{\mathrm{(bispicMe_2en)Mn(O)}\}_2]^{3+}$	III,IV	320	2.678	1.846, 1.853	94.5, 94.7	28
$[\mathrm{Mn_2O_2\{bispicMe_2(-)chxn\}_2}]^{3+}$	III,IV	293	2.693	1.855, 1.860	94.4, 95.1	28
$[\mathrm{Mn_2O(OAc)(bpy)_2Cl_2}]$	III,III	8.2		1.777–1.788	124.3	28
$[\mathrm{Mn_2O(OAc)_2(bpy)_2(N_3)_2}]$	III,III	−6.8		1.802	122.0	28
$[\mathrm{Mn_2O(OAc)_2\{HB(pz)_3\}_2}]$	III,III	0.4/1.4	3.159	1.773	125.1	29
$[\mathrm{Mn_2O(OAc)_2(TMACN)_2}]^{2+}$	III,III	−18		1.81	120.9	30
$[\mathrm{Mn_2(bpmp)(OAc)_2}]^{2+}$	II,III	12	3.447	2.19, 1.90	114.4	31
$[\mathrm{Mn_2(bcmp)(OAc)_2}]^{2+}$	II,III	15.4		2.17, 1.96	112.1	31
$\mathrm{Mn_3O(OAc)_6(py)_3py}$	II,III	10.2	3.218–3.248	1.936	120.0	32
	III,III	16.6		1.936	120.027	
$[\mathrm{Mn_2(bpy)_2(biphen)_2(Hbiphen)}]$	II,III	−1.78	2.667	2.142, 2.112	97.1, 102.4	24
$[\mathrm{LMn_2Cl_2Br}] \cdot \mathrm{H_2O}$	II,III	3.4	3.168	1.931–2.386	102.5, 93.6	33
$[\mathrm{Mn_2(O_2CC_2F_5)_4(H_2O)_3(NITEt)_2}]$	II,II	3.3	3.739	2.214–2.228	114.6	34
$[\mathrm{Mn_2(OAc)OH(TMACN)}]^+$	II,II	36	3.351	2.053	109.4	35

* Abbreviations used: pic = pyridine-2-carboxylate; phen = 1,10-phenanthroline; TMACN = 1,4,7-trimethyl-1,4,7-triazacyclononane; bispicen = N,N'-bis(2-pyridylmethyl)ethane-1,2-diamine; $\mathrm{N_3}$-Opy = N,N-bis(2-pyridylmethyl)glycinate; Ac = acetyl; TACN = 1,4,7-triazacyclononane; bpy = 2,2'-bipyridyl; cyclen = 1,4,7,10-tetraazacyclododecane; bpea = ethylbis(2-pyridylmethyl)amine; $\mathrm{bispicMe_2en}$ = N,N'-dimethyl-N,N'-bis(2-pyridylmethyl)ethane-1,2-diamine; $\mathrm{bispicMe_2}(-)$chxn = N,N'-bis(2-pyridylmethyl)dimethylcyclohexylamine; pz = pyrazolyl; bpmp = 4-methyl-2,6-bis-(pyridylmethylamine)phenol; bcmp = 4-methyl-2,6-bis(1,4,7-triazacyclononane)phenol; biphen = biphenyl.
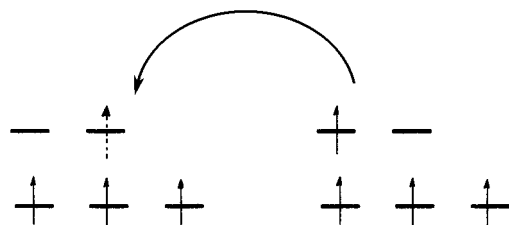
Fig. 3 Schematic representation of the spin dependent electron transfer in $\mathrm{Mn^{III}}$–$\mathrm{Mn^{IV}}$ pairs that originates the ferrromagnetic double exchange

Although in discrete molecular clusters the most common reported case is that of valence-trapped pairs, the delocalization of one electron can have a strong effect on the magnetic coupling, through the so-called double exchange. This in fact was first advocated in order to describe the magnetic properties of manganite perovskites,[36] which contain delocalized mananese(III) and manganese(IV) ions bridged by oxide ions. This effect is easily visualized considering the scheme shown in Fig. 3.

The unpaired electron in the σ* orbital of manganese(III) on the right can easily pass into the σ* orbital of manganese(IV) on the left provided that it maintains its spin. This generates a ferromagnetic coupling between the two sites, which is termed double exchange. Therefore there may be competition between the antiferromagnetic coupling determined by the superexchange and the ferromagnetic coupling associated with the double exchange. A convenient way of expressing the double exchange interaction is through a parameter B, which gives the energies of the S multiplets, doubled in number by the spin delocalization, equation (5). When B is large the S multiplet

$$E(S) = \pm B(S + \tfrac{1}{2}) \qquad (5)$$

with the maximum multiplicity lies lowest. Like all the phenomenological parameters B can be obtained through the

analysis of experimental data and it can be calculated through quantum mechanical methods. In particular B can often be obtained from the energy of the so-called intervalence transition. Recently Zhao *et al.*[37] reported density functional calculations of electronic structure, charge distribution, and spin coupling in manganese oxo dimer complexes. They considered $\mathrm{Mn^{III}_2}$, $\mathrm{Mn^{III}Mn^{IV}}$, and $\mathrm{Mn^{IV}_2}$ pairs and found satisfactory agreement with experiment.
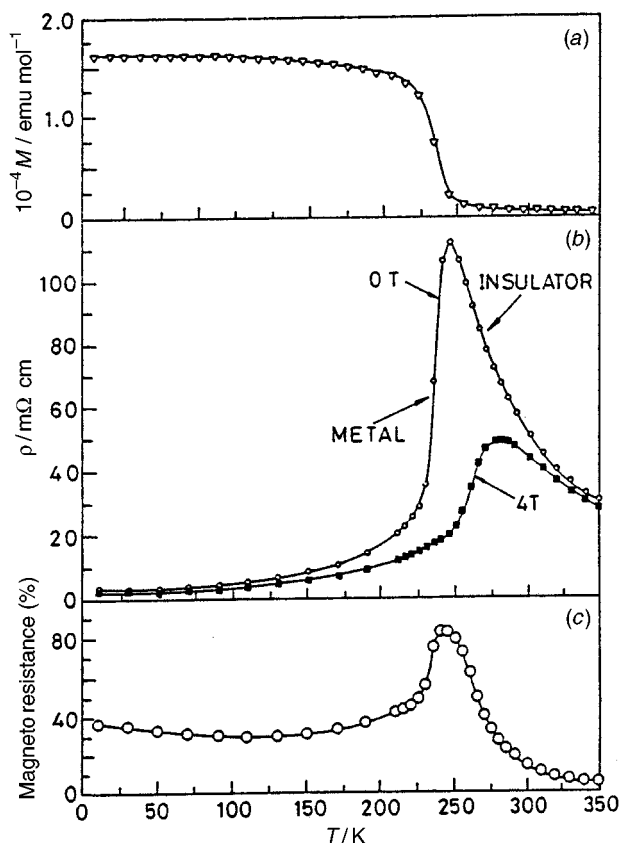
The double exchange has recently become of extreme importance because it has been observed in the manganite perovskites of general formula $\mathrm{La_{1-x}M^{II}_xMnO_3}$, which have been found to give rise to very large (colossal) variations in the resistance on application of moderately strong external magnetic fields.[7,8] Very broadly, in these compounds the fraction x of bivalent metal M introduces an analogous fraction of manganese(IV). For low values of x the manganese(III) and manganese(IV) are localized, and the compound behaves like an insulator, which eventually orders as an antiferromagnet at low temperature. On increasing x the fraction of manganese(IV) increases, and the mixed valences tend to delocalize. When the delocalization is strong the compound behaves like a metal and double exchange makes it ferromagnetic. Fig. 4 shows the temperature dependence of the resistance for $\mathrm{La_{0.75}Ca_{0.25}MnO_3}$ in the absence of an applied field. The sharp change in the resistance at *ca.* 250 K is due to the transition from the paramagnetic insulator to the ferromagnetic metal state. If the resistance is measured in an applied field of 4 T the transition is seen to occur at higher temperature: it is apparent that the application of the field favours the transfer of one electron from a manganese(III) to a neighbouring manganese(IV) ion, thus determining a dramatic drop in the resistance. The unique behaviour of manganites is associated with the interplay of Jahn–Teller distortions at the manganese(III) sites and double exchange interactions. They show again the enormous possibilities for anomalous behaviour for systems in which degenerate states are present.

The fact that charge localization is generally observed in

Table 2 Magnetic properties and structural types of tetranuclear manganese clusters

Compound	Ref.	Structure*	Ground state	Zero field splitting
$[Mn^{III}_3Mn^{IV}O_3X]^{6+}$	42	**d**	9/2	−0.3
$[Mn^{II}_2Mn^{III}_2O_2(OAc)_6(bipy)_2]$	43	**b**	2	
$[Mn^{III}_3Mn^{IV}O_2(O_2CPh)_7(pic)_2]$	44	**c**		

* See Fig. 5.

Fig. 5 Schematic view of the most common structural types of tetranuclear manganese clusters
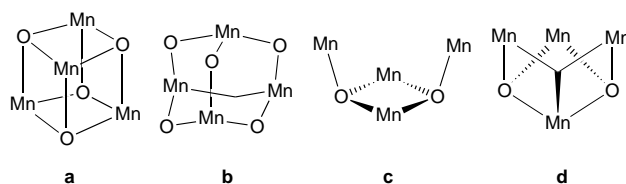

Fig. 4 Temperature dependence of (*a*) magnetization, (*b*) electrical resistivity in $H = 0$ T and $H = 4$ T, respectively, and (*c*) magnetoresistance in $La_{0.75}Ca_{0.25}MnO_3$ (after ref. 7)

clusters, while relatively numerous examples of charge delocalization are observed in infinite lattices, must be associated with the intrinsic low symmetry of the clusters where the presence of additional ligands beside oxide favour localization. Another important factor is the rigidity of the ionic lattices which favours delocalization.

Magnetic Properties of Tetranuclear Clusters

Tetranuclear clusters are the most investigated, because they are expected to behave as models of the water oxidizing complex, WOC. Several model complexes have been claimed to be useful to describe the structure of the different states of WOC. These are conventionally labelled as S_0–S_4, according to the nomenclature originally suggested by Kok *et al.*[38] The different states correspond to successive one-electron oxidations. The last state, S_4, is very short lived and it immediately releases oxygen, and reverts to S_0. In the model developed by Brudvig and Crabtree[39] the S_0–S_2 states correspond to cubane structures, Mn_4O_4, which shift to an adamantane structure, Mn_4O_6, in S_3–S_4. Alternatively Christou and Vincent[40] suggest a butterfly structure for S_0–S_2, shifting to an open cubane structure for S_3–S_4. An up to date discussion of the various models has been recently reported.[41] These structural types are shown in Fig. 5. The oxidation states of the clusters are still an open problem. One

possibility is that S_0 corresponds to (II,III$_3$), S_2 to (III$_3$,IV), and S_4 to (III$_2$,IV$_2$). The transition to S_3 seems not to be associated with manganese oxidation. An alternative based on X-ray excited Auger electron spectroscopy (XAS) data suggests that S_2 corresponds to (III$_3$,IV). In this case S_4 would correspond to (IV$_4$).

Entering the debate of WOC structure is absolutely beyond the objectives of the present contribution. Therefore here we will only show the magnetic properties of some tetranuclear mixed-valence manganese clusters which we find interesting. They are collected in Table 2.

The $[Mn^{III}_3Mn^{IV}O_3X]^{6+}$ ions have been intensively investigated[42] because of their open cubane structure, with a halide anion occupying the missing vertex. Their magnetic properties are dominated by the antiferromagnetic interactions between the manganese(IV) and the manganese(III) ions, which yield a ground state $S = \frac{9}{2}$ as a result of the $S_{III} = 6$ intermediate spin, which coupled to $S_{IV} = \frac{3}{2}$ in fact gives $S = \frac{9}{2}$. The spin arrangement of the cluster was attributed to spin frustration effects. However this is not the case, because the three manganese(III) spins in the triangle are ferromagnetically coupled. It would be more appropriate to talk of a ferromagnetic spin arrangement determined by the antiferromagnetic interaction between the manganese(III) and manganese(IV) ions.

There is a whole series of these compounds, with similar magnetic properties. A typical example is X = Cl, whose magnetic properties were fitted with $J_{III-IV} = 53.2$ and $J_{III-III} = -24.2$ cm^{-1}. Further a zero field splitting $D = -0.32$ cm^{-1} had to be included in order to fit the low-temperature magnetization data. Some confirmation to these values came from the frozen solution X-band EPR spectra which showed features at $g \approx 2$, 6 and 9. No simulation was attempted, but we have now made it finding that the qualitative aspect of the spectra can be satisfactorily reproduced, thus confirming the assignment. However the sign of the zero field splitting remains a puzzle. The ground state $S = \frac{9}{2}$ is given by the coupling of $S_{III} = 6$ and $S_{IV} = \frac{3}{2}$. Under these conditions, vector coupling techniques suggest[45] that the zero field splitting tensor is given by equation (6), where $D_{Mn^{III}}$

$$D_{9/2} = 3 \times 0.1446 D_{Mn^{III}} \tag{6}$$

is the single ion zero field splitting of one manganese(III) ion. Equation (6) is a tensorial relation, and the zero field splitting of the cluster is expected to have axial symmetry. The component parallel to the trigonal axis is then calculated to be: $D_{9/2,zz} = 3 \times 0.1446 (\sin^2 \theta \ D_{Mn^{III},xx} + \cos^2 \theta \ D_{Mn^{III},zz})$, where θ is the angle between the trigonal axis and the principal axis of the zero field splitting tensor of the individual manganese(III) ion. Since these have an elongated octahedral co-ordination, $D_{Mn^{III},zz}$ is expected to be negative and $D_{Mn^{III},xx} \approx -\frac{1}{2} D_{Mn^{III},zz}$, therefore for $θ \approx 109.47°$, $D_{9/2,zz}$ would be expected to be positive, contrary to observation.

Qualitatively the ferromagnetic coupling between the manganese(III) spins can be justified by the orbital overlap shown in Fig. 6, in agreement with the mechanism described in the previous sections. The antiferromagnetic coupling between manganese(III) and manganese(IV) ions, bridged by two oxo groups, is determined by the π interaction of the t_{2g} magnetic orbitals and perhaps also by direct interaction. In fact the Mn^{III}–Mn^{IV} distances are rather short (2.7–2.8 Å) suggesting some overlap between the magnetic orbitals.

Table 3 Structural types and magnetic properties of large Mn_n ($n > 4$) manganese clusters *

Compound	Ref.	Structure	Ground state
$n = 5$			
$[Mn^{II}\{Mn^{III}(sal)\}_4(OAc)_2(dmf)_6]$	47	**5a**	
$n = 6$			
$[Mn^{II}_4Mn^{III}_2(O_2CPh)_{10}(py)_2(MeCN)_2]$	48	**6a**	0
$[Mn^{II}_4Mn^{III}_2(O_2CPh)_{10}(py)_4]$	48	**6a**	0
$[Mn^{II}_4Mn^{III}_2(O_2CPh)_{10}(EtOH)_4(H_2O)]$	49	**6a**	0
$[Mn^{II}_4Mn^{III}_2(O_2CBu^t)_{10}(py)_4]$	50	**6a**	0
$[Mn^{III}_4Mn^{IV}_2(3,2,3\text{-}tet)_4O_6(OAc)_3]^{5+}$	51	**6b**	
$n = 7$			
$[Mn^{II}Mn^{III}_6(trien)_2(dien)_2O_4(OAc)_8]^{4+}$	52	**7a**	
$[Mn^{II}_3Mn^{III}_4(OH)_3Cl_3(hmp)_9]^{2+}$	53	**7b**	$\geqslant 10$
$n = 8$			
$[Mn^{II}_2Mn^{III}_6O_4(O_2CPh)_{12}(Et_2mal)_2(H_2O)]^{2-}$	54	**8a**	3
$n = 9$			
$[Mn^{II}Mn^{III}_8O_4(O_2CPh)_8(sal)_4(Hsal)_2(py)_4]$	55	**9a**	0
$n = 10$			
$[Mn^{II}_6Mn^{III}_4O_4(biphen)_4X_{12}]^{4-}$	56	**10a**	12
$[Mn^{II}_2Mn^{III}_8O_2Cl_8\{(OCH_2)_3CMe\}_6]$	57	**10b**	
$[Mn^{III}_4Mn^{IV}_6O_{14}(tren)_6]^{8+}$	58	**10c**	
$n = 12$			
$[Mn^{III}_8Mn^{IV}_4O_{12}(OAc)_{16}(H_2O)_4]$	59	**12a**	10
$[Mn^{III}_8Mn^{IV}_4O_{12}(O_2CPh)_{16}(H_2O)_4]$	60	**12a**	9
$[Mn^{II}Mn^{III}_7Mn^{IV}_4O_{12}(O_2CPh)_{16}(H_2O)_4]^-$	61	**12b**	19/2
$[Mn^{II}Mn^{III}_7Mn^{IV}_4O_{12}(O_2CEt)_{16}(H_2O)_4]^-$	62	**12b**	19/2
$[Mn^{III}_4Mn^{IV}_4Fe^{III}_4O_{12}(OAc)_{16}(H_2O)_4]$	62	**12c**	

* Abbreviations used: Hsal = salicyclaldehyde; dmf = dimethylformamide; 3,2,3-tet = N,N'-bis(3-aminopropyl)ethane-1,2-diamine; trien = triethylene-tetraamine; dien = diethylenetriamine; hmp = 2-hydroxymethylpyridine; Et_2mal = pentane-3,3-dicarboxylate; tren = tris(2-aminoethyl)amine.
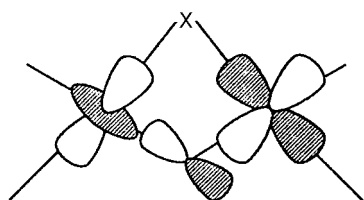
Fig. 6 Schematic drawing of the overlap of the magnetic orbitals in the oxo-bridged Mn^{III}–Mn^{IV} pairs with the open cubane structure

An interesting feature of the magnetic properties of these clusters at low temperature has recently been reported.[46] The large spin in the ground state, associated with the relatively large zero field splitting gives rise to a high barrier for the re-orientation of the magnetization. In fact, in axial symmetry the ground state is split leaving the $M = \pm\frac{9}{2}$ components lying lowest. When the cluster is in the $+\frac{9}{2}$ state the magnetization is up, when it is in the $-\frac{9}{2}$ state the magnetization is down. The passage from $+\frac{9}{2}$ to $-\frac{9}{2}$ (which corresponds to inverting the direction of the magnetization) cannot be performed directly, because the $+\frac{9}{2} \longrightarrow -\frac{9}{2}$ transition is forbidden. The system must climb the ladder of levels from $+\frac{9}{2}$ to $+\frac{7}{2}$, then to $\frac{5}{2}$, and so on up to $+\frac{1}{2}$ and then descend all the way down to $-\frac{9}{2}$. This can occur with a thermally excited process, with an effective barrier corresponding to the energy separation between $+\frac{9}{2}$ and $\frac{1}{2}$, i.e. $(-81/4 + 1/4)D \approx 6$ cm^{-1}. The relaxation time of the magnetization is expected to depend on temperature as shown in equation (7),

$$\tau = \tau_0 \exp(-\Delta/kT) \qquad (7)$$

where $\Delta = 6$ cm^{-1}. In fact low-temperature a.c. susceptibility measurements have shown that the relaxation time of the magnetization at 1.7 K is ca. 7×10^{-4} s.

Magnetic Properties of Larger Clusters

The structural types and the magnetic properties of a few mixed-valence manganese clusters are shown in Table 3 and Fig. 7. It is apparent that a large number of ground states is possible, including some with very high spin. So far the cluster
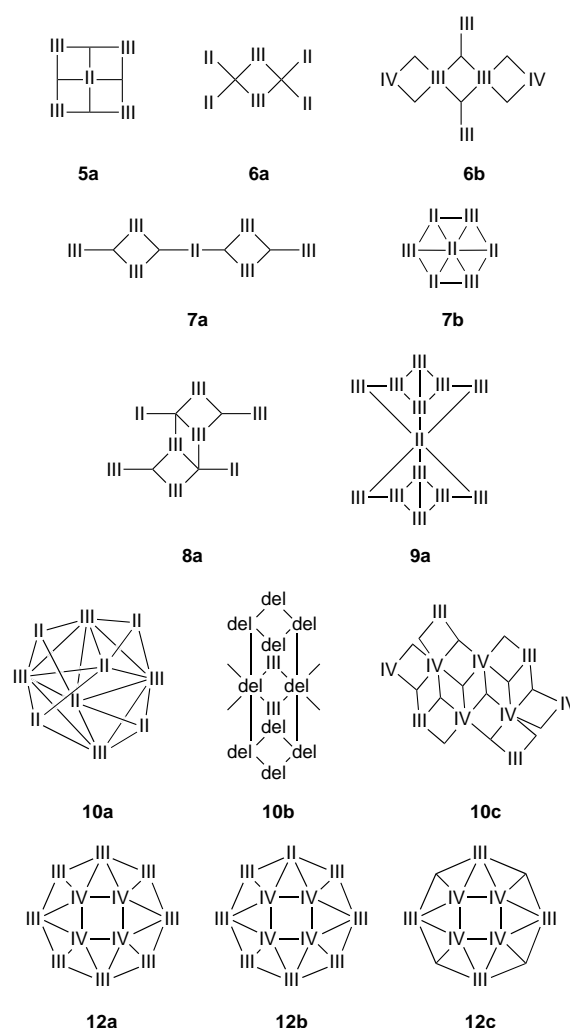
Fig. 7 Scheme of the structural types of manganese clusters with more than four metal ions (del in **10b** stands for delocalized)
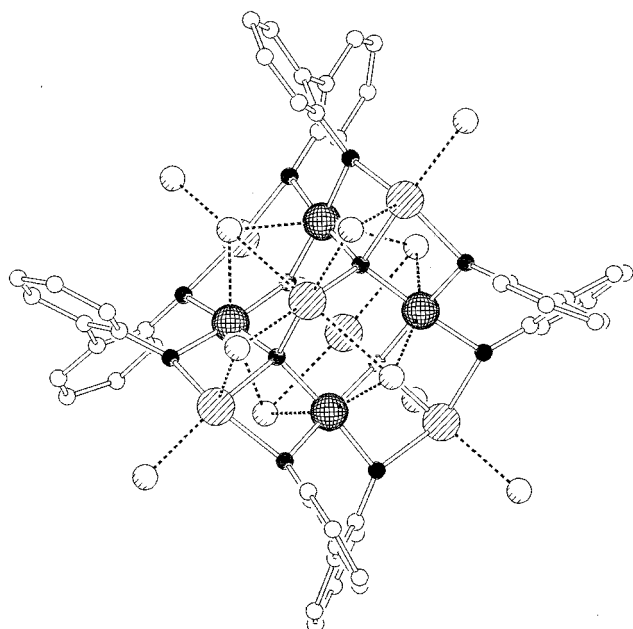
Fig. 8 Structure of the $[Mn^{II}_6Mn^{III}_4O_4(biphen)_4X_{12}]^{4-}$ cluster

Fig. 9 High frequency EPR spectrum of a polycrystalline powder of $[Mn^{II}_6Mn^{III}_4O_4(biphen)_4X_{12}]^{4-}$ at 245 GHz and four different temperatures. (*a*) Experimental, (*b*) simulation with the parameters reported in the text

Fig. 10 Spin topology and spin structure of $[Mn^{II}_6Mn^{III}_4O_4(biphen)_4X_{12}]^{4-}$

with the largest ground state spin is $[Mn^{II}_6Mn^{III}_4O_4(biphen)_4X_{12}]^{4-}$, whose structure[56] is shown in Fig. 8. An adamantane-like inner core comprising two manganese(II) and four manganese(III) ions is connected through the four oxygen atoms to four manganese(II) ions. The χT product for the chloride derivative steadily increases from the room temperature value of 37.9 K emu mol^{-1} to 95 K emu mol^{-1} at 5 K. The former value corresponds to that expected for uncoupled ions, while the low-temperature value suggests a ground state with $S \geqslant 12$. The exact value of the ground state is difficult to determine because the compound crystallizes with CH_2Cl_2 which is only loosely bound, and can give errors in the molar susceptibility. Further ferromagnetic intermolecular interactions may be present, which give a χT value larger than expected for non-interacting clusters. In fact the low-temperature data could be fitted to a Curie–Weiss law, with $C = 82$ K emu mol^{-1} and $\theta = 0.40$ K. The Curie constant is closer to the limit expected for $S = 12$ (78 K emu mol^{-1}) than to that for $S = 13$ (91 K emu mol^{-1}). An unambiguous assignment could be obtained from the HF-EPR spectra,[63] shown in Fig. 9. The spectra were recorded at an exciting frequency of 245 GHz, with temperatures ranging from 50 to 4.5 K. In this case the polarization effects of the transitions due to the fact that the Zeeman energy is comparable to thermal energy at low temperature are quite apparent. In fact the relative intensities of the outermost features, both at low and high field, dramatically increase on decreasing temperature. This is due to the fact that at low temperature only the lowest lying $M = -S$ component of the S multiplet is thermally populated. The parallel transition $-S \longrightarrow -S + 1$ occurs at low field when the zero field splitting is negative, and at high field when the zero field splitting is positive. The spectra of Fig. 9 clearly show that the zero field splitting is negative in $[Mn^{II}_6Mn^{III}_4O_4(biphen)_4X_{12}]^{4-}$, because the low field feature seen in the spectrum recorded at 4 K is clearly a parallel transition. The resonance fields are easily computed in the strong field limit for axial symmetry, equation (8). The spectra could be simulated using $S = 12$ and

$$H_z = \frac{g_e}{g_z}[H_0 + (2S - 1)D]; \; H_{x,y} = \frac{g_e}{g_{x,y}}\left[H_0 - \frac{(2S - 1)D}{2}\right] \quad (8)$$

$S = 13$, but only with the former value acceptable g parameters were found. The best fit values are: $g_z = 1.974$, $g_{x,y} = 1983$, $D = -0.047$ cm^{-1}. It should be mentioned that the small value of the zero field splitting parameter allowed the spectra to also

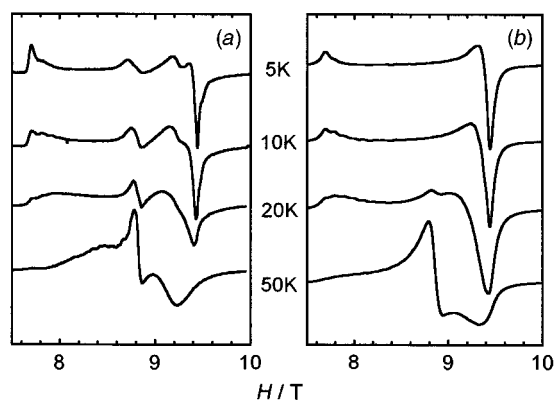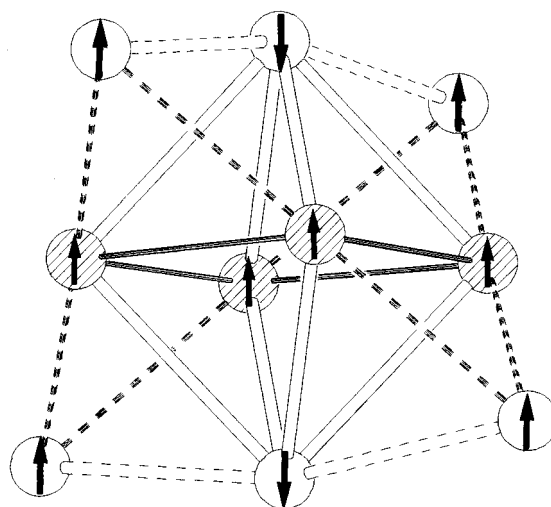be recorded at X-band frequencies, but no satisfactory conclusion on the nature of the ground state could be reached.

The information which can be extracted from the above data is that the anisotropy in the cluster is dominated by the single ion anisotropy of the manganese(III) ions. The observed negative zero field splitting is the result of the single ion zero field splitting of the manganese(III) ions, which have a tetragonally elongated structure, analogous to that observed in $[Mn(dbm)_3]$ reported above.[11] Also the pattern of g values, with $2 > g_{x,y} > g_z$ agrees with the g values of the individual manganese(III) ions. The quantitative analysis of the temperature dependence of the magnetic susceptibility is very difficult to perform due to the very large number of states $(2.5 + 1)^6(2.2 + 1)^4$ originating from the interaction between the ten manganese ions. However a qualitative indication of the nature of the ground state can be suggested using the diagram of spin topology of Fig. 10. If the four manganese(III) ions have their spins parallel to each other, the result is $S_{III} = 8$. The manganese(II) spins S_7–S_{10} are parallel to each other and antiparallel to the S_5 and S_6, to give a resulting $S_{II} = 5$. The maximum total spin can be $S = 13$, but in the presence of spin frustration lower S values are also admitted, *e.g.* $S = 12$.

These speculations can find some justification from an experimental determination of the unpaired spin density obtained through polarized neutron experiments. It is well known that neutron scattering can be used to determine the magnetic structure of ordered materials, like ferro- and antiferro-magnets.[64] Similar results can be obtained also for paramagnets if the experiments are performed in the presence
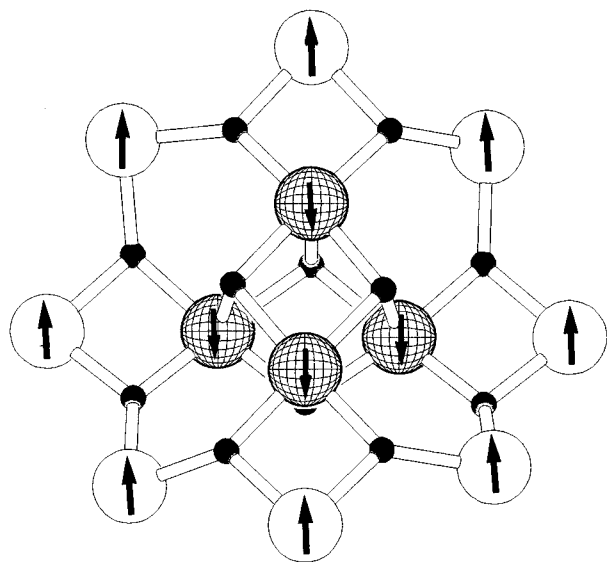
Fig. 11 View of the structure of the core of the $[Mn_{12}O_{12}(OAc)_{16}(H_2O)_4]$ cluster

of an applied field at sufficiently low temperature to determine a difference in population large enough between the different M levels. The neutron beam can be circularly polarized, either left or right, and the two polarizations will interact differently with the $+M$ and $-M$ state of the paramagnet. Through an analysis of the polarized diffraction data it is possible to map the unpaired spin density on the molecule. The results of such an analysis [65] for $[Mn^{II}_6Mn^{III}_4O_4(biphen)_4X_{12}]^{4-}$ show that indeed the spin density at the manganese(III) sites is positive, and so is the spin density of four manganese(II) sites, while it is reversed on the other two manganese(II) sites, in agreement with the simplified qualitative model above. The quantitative analysis of the spin densities suggests a ground state smaller than $S = 13$.

Another class of clusters with a large ground spin state, which have attracted attention for their unique properties at very low temperatures is that which has $[Mn^{III}_8Mn^{IV}_4O_{12}(O_2-Ac)_{16}(H_2O)_4]$ as the first example.[64] The structure of this compound was reported [59] in the early 80s and is shown in Fig. 11. There is an external ring of eight manganese(III) ions, which are bridged to an internal tetrahedron of manganese(IV) by oxo bridges. It is interesting to note that while there is so far no report of tetranuclear clusters with the cubane Mn_4O_4 structure, this is stabilized in the core of the $[Mn^{III}_8Mn^{IV}_4O_{12}(OAc)_{16}(H_2O)_4]$ cluster. The temperature dependence of the magnetic susceptibility clearly shows that the cluster behaves in a ferrimagnetic way, with χT at room temperature of *ca.* 19 K emu mol^{-1} which goes through a broad minimum at *ca.* 200 K and then increases to *ca.* 56 K emu mol^{-1} at 20 K. These values, together with magnetization data clearly showed [64] that the ground state has $S = 10$, which can be easily rationalized by a spin structure in which the manganese(III) spins are all parallel to each other to give $S_{III} = 16$ and the manganese(IV) spins are also parallel to each other to give $S_{IV} = 6$. The two sets of spins are antiparallel to each other to give the observed $S = 10$ ground state. The origin of the ground state is due to the fact that the manganese(III)–manganese(IV) interactions mediated by bis(μ-oxo) bridges are strongly antiferromagnetic and they dominate the complex pattern of interactions. The remarkable magnetic properties of $[Mn^{III}_8Mn^{IV}_4O_{12}(OAc)_{16}(H_2O)_4]$ are observed [5b] below 10 K, and they are associated with the large zero field splitting of the ground $S = 10$ multiplet. In fact the elongation axes of the distorted manganese(III) ions are closely parallel to each other, in such a way that the single ion zero field splitting gives a strong resultant in the $S = 10$ ground state. The value of D has been estimated to be in the range ± 0.4–0.5 cm^{-1} from different techniques ranging from HF-EPR to inelastic

neutron scattering. The large and negative zero field splitting gives rise to a large barrier for the reorientation of the magnetization as outlined above for $[Mn^{III}_3Mn^{IV}O_3X]$. At low temperature the relaxation becomes extremely slow. It has been found to follow a thermally activated law with $\tau_0 = 2.1 \times 10^{-7}$ s, and $D/k = -0.42$ K. This means that at 2 K the clusters behave as magnets, single-molecule magnets. This unique behaviour is dramatically evidenced by the observation of magnetic hysteresis in frozen solution. Recently Thomson and co-workers [66] reported that the magnetic hysteresis can also be optically detected through magnetic circular dichroism measurements.

Below 2 K the relaxation of the magnetization becomes independent of temperature, suggesting that it may occur through a tunnelling mechanism.[67] However, tunnelling also occurs at higher temperatures, as shown [6] by the stepped hysteresis loops observed in the range 2–4 K. These clusters open exciting perspectives for observing quantum phenomena in mesoscopic matter and for developing quantum computers.

Acknowledgements

References

1 G. C. Dismukes, in '*Mixed Valency Systems: Applications in Chemistry, Physics and Biology*', ed. K. Prassides, Kluwer, Dordrecht, 1990.
2 G. C. Dismukes, *Photochem. Photobiol.*, 1986, **43**, 99.
3 W. F. Beyer and I. Fridovich, *Biochemistry*, 1985, **24**, 6360.
4 A. Willing, H. Follmann and G. Auling, *Eur. J. Biochem.*, 1988, **170**, 603.
5 (*a*) D. Gatteschi, A. Caneschi, L. Pardi and R. Sessoli, *Science*, 1994, **265**, 1065; (*b*) R. Sessoli, D. Gatteschi, A. Caneschi and M. Novak, *Nature (London)*, 1993, **365**, 141.
6 L. Thomas, F. Lionti, R. Ballou, D. Gatteschi, R. Sessoli and B. Barbara, *Nature (London)*, 1996, **383**, 145; J. Friedman, M. P. Sarachik, J. Tejada, J. Maciejewski and R. Ziolo, *Phys. Rev. Lett.*, 1996, **76**, 3820.
7 C. N. Rao, *Chem. Eur. J.*, 1996, **2**, 1499.
8 K. Chahara, T. Ohno, M. Kasi and K. Yozono, *Appl. Phys. Lett.*, 1993, **63**, 1990.
9 S. L. Dexheimer, J. W. Gohdes, M. K. Chan, K. S. Hagen, W. H. Armstrong and M. P. Klein, *J. Am. Chem. Soc.*, 1989, **111**, 8923.
10 M. P. Hendrick and P. F. Debrunner, *J. Magn. Reson.*, 1988, **78**, 133.
11 A. L. Barra, D. Gatteschi, R. Sessoli, G. L. Abbati, D. Cornia, A. C. Fabretti and M. G. Uytterhoeven, *Angew. Chem., Int. Ed. Engl.*, in the press.
12 J. S. Griffith, *The Theory of Transition Metal Ions*, Cambridge University Press, Cambridge, 1964.
13 A. B. P. Lever, *Inorganic Electronic Spectroscopy*, Elsevier, Amsterdam, 1984.
14 A. Abragam and M. H. L. Pryce, *Proc. R. Soc. London, Ser. B*, 1951, **206**, 13.
15 H. J. Gerritsen and E. S. Sabisky, *Phys. Rev.*, 1963, **132**, 1507.
16 M. Zheng, G. C. Dismukes, *Inorg. Chem.*, 1996, **35**, 3307.
17 J. B. Goodenough, *Phys. Rev.*, 1955, **100**, 654; J. Kanamori, *J. Phys. Chem. Solids*, 1959, **10**, 87.
18 E. Libby, R. J. Webb, W. E. Streib, K. Folting, J. C. Huffmann, D. N. Hendrickson and G. Christou, *Inorg. Chem.*, 1989, **28**, 4037.
19 M. Stebler, A. Ludi and H. B. Bürgi, *Inorg. Chem.*, 1986, **25**, 4743.
20 K. Wieghardt, U. Bossek, B. Nuber, J. Weiss, J. Bonvoisin, M. Corbella, S. E. Vitals and J.-J. Girerd, *J. Am. Chem. Soc.*, 1988, **110**, 7398.
21 E. S. Dodsworth and A. B. P. Lever, *Inorg. Chem.*, 1990, **29**, 699.
22 M. Suzuki, H. Senda, Y. Kobayashi, H. Oshio and A. Uehara, *Chem. Lett.*, 1988, 1763.
23 K. Wieghardt, U. Bossek, L. Zsolnai, G. Huttner, G. Blondin, J.-J. Girerd and F. Babonneau, *J. Chem. Soc., Chem. Commun.*, 1987, 651.
24 J. S. Bashkin, A. R. Schake, J. B. Vincent, H.-R. Chang, Q. Li, J. C. Huffman, G. Christou and D. N. Hendrickson, *J. Chem. Soc., Chem. Commun.*, 1988, 700.

25 S. R. Cooper, G. C. Dismukes, M. P. Klein and M. Calvin, *J. Am. Chem. Soc.*, 1977, **99**, 6623.

26 P. A. Goodson, D. J. Hodgson, J. Glerup, K. Michelsen and H. Weihe, *Inorg. Chim. Acta*, 1992, **197**, 141.

27 S. Pal, M. M. Olmstead and W. H. Armstrong, *Inorg. Chem.*, 1995, **34**, 4708.

28 A. R. Schake, J. B. Vincent, Q. Li, P. D. W. Boyd, K. Folting, J. C. Huffmann, D. N. Hendrickson and G. Christou, *Inorg. Chem.*, 1989, **28**, 1915.

29 J. E. Sheats, R. S. Czernuszewicz, G. C. Dismukes, A. L. Rheingold, V. Petrouleas, J. Stubbe, W. H. Armstrong, R. H. Beer and J. S. Lippard, *J. Am. Chem. Soc.*, 1987, **109**, 1435.

30 K. Wieghardt, U. Bossek, D. Ventur and J. Weiss, *J. Chem. Soc., Chem. Commun.*, 1985, 347.

31 H. Diril, H.-R. Chang, S. K. Larsen, J. A. Potenza, C. G. Pierpont, H. J. Schugar, S. S. Isied and D. N. Hendrickson, *J. Am. Chem. Soc.*, 1987, **109**, 6207.

32 J. B. Vincent, H.-R. Chang, K. Folting, J. C. Huffman, G. Christou and D. N. Hendrickson, *J. Am. Chem. Soc.*, 1987, **109**, 5703.

33 H.-R. Chang, S. K. Larsen, P. D. W. Boyd, C. G. Pierpont and D. N. Hendrickson, *J. Am. Chem. Soc.*, 1988, **110**, 4565.

34 A. Caneschi, F. Ferraro, D. Gatteschi, M. C. Melandri, P. Rey and R. Sessoli, *Angew. Chem., Int. Ed. Engl.*, 1989, **28**, 1365.

35 K. Wieghardt, U. Bossek, J. Bonvoisin, P. Beauvillain, J. J. Girerd, B. Nuber, J. Weiss, and J. Heinze, *Angew. Chem., Int. Ed. Engl.*, 1986, **25**, 1030.

36 C. Zener, *Phys. Rev.*, 1951, **82**, 403; P. W. Anderson and H. Hazegawa, *Phys. Rev.*, 1955, **100**, 675.

37 X. G. Zhao, W. H. Richardson, J.-L. Chen, J. Li, L. Noodleman, H.-L. Tsai and D. N. Hendrickson, *Inorg. Chem.*, 1997, **36**, 1198.

38 B. Kok, B. Forbush and M. McGloin, *Photochem. Photobiol.*, 1970, **11**, 457.

39 G. W. Brudvig and R. H. Crabtree, *Proc. Natl. Acad. Sci. USA*, 1986, **83**, 4586.

40 G. Christou and J. B. Vincent, *Biochim. Biophys. Acta*, 1987, **895**, 259.

41 V. K. Yachandra, K. Sauer and M. P. Klein, *Chem. Rev.*, 1996, **96**, 2927.

42 D. N. Hendrickson, G. Christou, E. A. Schmitt, E. Libby, J. S. Bashkin, S. Wang, H.-L. Tsai, J. B. Vincent, P. D. W. Boyd, J. C. Huffman, K. Folting, Q. Li and W. Streib, *J. Am. Chem. Soc.*, 1992, **114**, 2455.

43 J. B. Vincent, C. Christmas, H.-R. Chang, Q. Li, P. D. W. Boyd, J. C. Huffman, D. N. Hendrickson and G. Christou, *J. Am. Chem. Soc.*, 1989, **111**, 2086.

44 E. Libby, J. K. McCusker, E. A. Schmitt, K. Folting, D. N. Hendrickson and G. Christou, *Inorg. Chem.*, 1991, **30**, 3486.

45 A. Bencini and D. Gatteschi, *EPR of Exchange Coupled Systems*, Springer, Berlin, 1990.

46 S. M. J. Aubin, M. W. Wemple, D. M. Adams, H.-L. Tsai, G. Christou and D. N. Hendrickson, *J. Am. Chem. Soc.*, 1996, **118**, 7746.

47 M. S. Lah and V. L. Pecoraro, *J. Am. Chem. Soc.*, 1989, **111**, 7258.

48 A. R. Schake, J. B. Vincent, Q. Li, P. D. W. Boyd, K. Folting, J. C. Huffman, D. N. Hendrickson and G. Christou, *Inorg. Chem.*, 1989, **28**, 1917.

49 A. G. Blackman, J. C. Hufman, E. B. Lobkovsky and G. Christou, *Polyhedron*, 1992, **11**, 251.

50 K. Köhler, H. W. Roesky, M. Noltemeyer, H.-G. Schmidt, C. Freire-Erdbrügger and G. M. Sheldrick, *Chem. Ber.*, 1993, **126**, 921.

51 R. Bhula, S. Collier, W. T. Robinson and D. C. Weatherburn, *Inorg. Chem.*, 1990, **29**, 4027.

52 R. Bhula and D. C. Weatherburn, *Angew. Chem., Int. Ed. Engl.*, 1991, **30**, 688.

53 M. A. Bolcar, S. M. J. Aubin, K. Folting, D. N. Hendrickson and G. Christou, *Inorg. Chem.*, in the press.

54 M. W. Wemple, H.-L. Tsai, W. E. Streib, D. N. Hendrickson and G. Christou, *J. Chem. Soc., Chem. Commun.*, 1994, 1031.

55 D. W. Low, D. M. Eichhorn, A. Draganescu and W. H. Armstrong, *Inorg. Chem.*, 1991, **30**, 877.

56 D. P. Goldberg, A. Caneschi, C. D. Delfs, R. Sessoli and S. J. Lippard, *J. Am. Chem. Soc.*, 1995, **117**, 5789.

57 M. Cavaluzzo, Q. Chen and J. Zubieta, *J. Chem. Soc., Chem. Commun.*, 1993, 131.

58 K. S. Hagen, W. H. Armstrong and M. M. Olmstead, *J. Am. Chem. Soc.*, 1989, **111**, 774.

59 T. Lis, *Acta Crystallogr., Sect. B*, 1980, **36**, 2042.

60 P. D. W. Boyd, Q. Li, J. B. Vincent, K. Folting, H.-R. Chang, W. E. Streib, J. C. Huffman, G. Christou and D. N. Hendrickson, *J. Am. Chem. Soc.*, 1988, **110**, 8537.

61 H.-L. Tsai, H. J. Eppley, N. de Vries, K. Folting, G. Christou and D. N. Hendrickson, *J. Chem. Soc., Chem. Commun.*, 1994, 1745.

62 A. R. Schake, H.-L. Tsai, N. de Vries, R. J. Webb, K. Folting, D. N. Hendrickson and G. Christou, *J. Chem. Soc., Chem. Commun.*, 1992, 181.

63 A.-L. Barra, A. Caneschi, D. Gatteschi and R. Sessoli, *J. Am. Chem. Soc.*, 1995, **117**, 8855.

64 R. Sessoli, H.-L. Tsai, A. R. Schake, S. Wang, J. B. Vincent, K. Folting, D. Gatteschi, G. Christou and D. N. Hendrickson, *J. Am. Chem. Soc.*, 1993, **115**, 1804.

65 A. Caneschi, D. Gatteschi, R. Sessoli and J. Schweizer, unpublished work.

66 M. R. Cheeseman, V. Oganesyan, R. Sessoli, D. Gatteschi and A. J. Thomson, *Chem. Commun.*, in the press.

67 M. A. Novak and R. Sessoli, in *Quantum Tunneling of the Magnetization*, eds. L. Gunther and B. Barbara, *NATO-ASI Ser., Ser. E*, Kluwer, Dordrecht, 1995, vol. 301.